Palm Kernel Shell Activated Carbon for Lead and Methylene Blue Removal

Decklary Jawing, Syahriadi Syahril, Mohd Hardyianto Vai Bahrun, Rachel Fran Mansa#

Faculty of Engineering, Universiti Malaysia Sabah, Jalan UMS, 88400 Kota Kinabalu, Sabah, MALAYSIA.
#Corresponding author. E-Mail: rfmansa@ums.edu.my; Tel: +6088-320000 ext: 1543; Fax: +6088-320348.

ABSTRACT Palm kernel shell activated carbon (PKSAC) is a porous material with high surface area used in adsorption application. The abundance of palm kernel shells from palm oil mills attracted researchers to use them as a precursor for activated carbon. This research investigates the ability of PKSAC for lead ion (Pb^{2+}) and methylene blue (MB) removal. Two size of PKSACs (0.4 mm and 1.4 mm) were prepared through chemical activation with 50w/w% potassium hydroxide, followed by activation in tube furnace at 800°C, and named as 0.4-50 PKSAC and 1.4-50 PKSAC, respectively. Morphology of PKS biochar and PKSACs were observed using field emission scanning electron microscope (FESEM) to observe the surface characteristics. The PKSACs were characterized for their ash and moisture content, iodine number, pH, and bulk density. Then, the response surface methodology (RSM) employing Box-Behnken design, with three independent variables were used to construct the experimental design for batch adsorption study, with percentage removal as the response. The independent variables were initial concentration (5 – 20 ppm for Pb^{2+}, 50 – 250 ppm for MB), pH (4.5 – 7 for Pb^{2+}, 4 – 10 for MB) and contact time (20 – 60 min for Pb^{2+}, 60 – 120 min for MB). The interactive effect of the independent variables on the percentage removal of Pb^{2+} and MB by 0.4-50 PKSAC and 1.4-50 PKSAC were investigated using 3D surface plots. The highest experimental Pb^{2+} percentage removal by 0.4-50 PKSAC and 1.4-50 PKSAC was 98.20% and 95.48%, respectively, at conditions of initial concentration of 20 ppm, contact time of 60 min and pH 7. While the highest experimental MB percentage removal by 0.4-50 PKSAC and 1.4-50 PKSAC was 99.97% and 98.71%, respectively, at initial concentration of 50 ppm, contact time of 90 min and pH 10. Overall, the present study concludes the ability of PKSACs in removing Pb^{2+} and MB, with reported percentage removal of >95%.

KEYWORDS: Adsorption; Lead ion; Methylene blue; Palm kernel shell activated carbon; Response surface methodology
Received 26 November 2020 **Revised** 2 December 2020 **Accepted** 23 December 2020 **Online** 2 November 2021

Original Article

TRANSACTIONS ON SCIENCE AND TECHNOLOGY

INTRODUCTION

Heavy metals may come from various industrial processes such as galvanizing, and metal smelting which can become a water pollutant source (Huang *et al.*, 2016). Unregulated water discharge from the manufacturing industries can cause contamination in the rivers and seas. Even low concentrations of lead ion (Pb^{2+}) at 0.10 mg/L in drinking water can be harmful to humans because it can bio-accumulate in the long term, which can cause cancer. Meanwhile methylene blue was used for the dying of silk, leather, fabrics, paper, and cotton mordant with tannin, as well as to produce dye. But its use was a concern as it is a toxic substance and produces blue colourings in the water, as well as not easily biodegradable, since dyes have a synthetic origin and a complex molecular aromatic structure (Kumar *et al.*, 2011; Biswas & Mishra, 2015; García *et al.*, 2017).

Activated carbon can be made from a variety of raw material, for instance, sawdust, coconut shell, wood, bamboo, rice husk, sugarcane, and coal. However, in Malaysia, the palm oil industry accounts for 94% of biomass stock (Rahman *et al.*, 2016). Thus, resulting in a large amount of palm kernel shell (PKS) waste. But it has a high potential to be made into activated carbon because of its mechanical strength, porous surface, high chemical stability, different functional groups, and water insolubility (Rashidi & Yusup, 2019). Furthermore, PKS is cheaper and easier to collect as it is abundant locally (Mohamad Salleh, 2010). Due to the low cost, it is a suitable raw material for activated carbon for wastewater treatment. This ensures that the wastewater treatment process is environmentally friendly

and does not produce toxic pollutants. In addition to that activated carbon can be reused after the desorption process, by burning off the lead content from the carbon surface. The PKS biochar used in this study was formed through slow vacuum pyrolysis. According to Rugayah *et al.*, (2014), PKS biochar can be a source of raw material to produce activated carbon due to low ash content.

Activated carbon is mostly used for the treatment of wastewater. Saleem *et. al.* (2019) reported the activated carbon adsorption capacity is proportional to the internal surface area, pore volume, pore distribution and its surface chemistry. Its ability to adsorb depending on the activating chemical and the conditions of the application. Table 1. Examples of commercially available activated carbon was obtained by doing a review online of the companies that provide activated carbon, and it shows several types of commercially available activated carbon.

Table 1. Examples of commercially available activated carbon

Raw material	Type (mesh)/ Size (mm)	Iodine number (mg/g)	Methylene blue adsorption (mg/g)	Ash (%)	Bulk density (g/mL)	Hardness (%)	Moisture (%)	Company
Coal	-/2.5~1.2	950-1150	≥150	5-18	N/A	≥90	≤5.0	Shanxi Xinhua Chemical Co, Ltd
Wood	N/A	300-1300	N/A	1-40	0.35-0.65	85-98	0.5-8	Sincere
Coconut shell	N/A	>950	N/A	4-8	0.45-0.55	≥90	≤5.0	Ningqxia Baiyun Carbon
Coal based coconut shell	8-40/-	800-1400	120-170	≤5.0	0.5-0.6	≥95	≤8.0	XW Hebei, China
Coconut shell	N/A	900-1250	135-210	≤3.0	N/A	N/A	≤5.0	Zhenghou Kelin

This work is based on a previous work by Sinring (2019), which was on the response surface methodology optimization of PKS biochar activation using KOH to produce PKSAC. The parameters were particle size, activating temperature and KOH concentrations. The study reported that PKSAC with iodine number higher than 1100 mg/g, which is comparable to commercially available activated carbon, could be produced. Thus, this present work aims to investigate the ability of the PKSAC in lead ion (Pb^{2+}) and methylene blue (MB) removal. The ability of any activated carbon to remove heavy metal and dyes from wastewater can be affected by its iodine number, which is indirect measurement of porosity, and particle size, as well as the initial concentration of the pollutant, the pH of the solution and the contact time. Response surface methodology (RSM) through Box-Behnken design framework was used to construct the experimental sets, and to model the response of percentage removal of Pb^{2+} and MB with independent variables of initial concentration, pH and contact time, at two particle sizes of PKSAC.

METHODOLOGY

Chemicals and Materials

The palm kernel shell (PKS) biochar stock was supplied by Borneo Energy Sdn Bhd, Lahad Datu, Sabah. Potassium hydroxide (KOH), hydrochloric acid (HCl) and sodium thiosulphate ($Na_2S_2O_3 \cdot 5H_2O$) were supplied by ChemAR, SYSTERM. GradeAR supplied potassium iodide (KI) and starch soluble ($C_{27}H_{48}O_{20}$) (Qrec brand). Lead standard solution (Pb) and methylene blue (MB) were supplied by MERCK. Iodine soluble was purchased from Sigma-Aldrich.

Palm Kernel Shell (PKS) Biochar Particle Size Preparation

PKS biochar was grounded using a grinder (locally produced) and sieved using 420 and 1410 μm mesh size sieves (Unit Test Specific T20). The sieved PKS biochar was be referred to as 0.4 mm and 1.4 mm, respectively. The mass of sieved PKS biochar was recorded using a weighing balance (Shimadzu, TX42021). This PKS biochar with a specific size was prepared for chemical activation. The sieve sizes were selected based on the results of the previous work by Sinring (2019), which showed that these two sizes could produce activated carbon with iodine numbers higher than 1100 mg/g. The sieved PKS biochar were converted to PKS activated carbon through chemical activation.

Palm Kernel Shell (PKS) Activated Carbon Preparation

The PKS biochar was converted to PKS activated carbon via chemical activation. The conditions of chemical activation of PKS biochar follows the technique of the work by Sinring (2019), as the conditions produced activated carbon with iodine number greater than 1100 mg/g. Potassium hydroxide (KOH) solution with 50w/w% concentration was poured into a beaker containing 100 g of 0.4 mm sized PKS biochar and was stirred to ensure homogeneity between PKS biochar and the activating agent. The sample was wrapped with aluminum foil and allowed to soak for 24 hours. Then, the PKS biochar-soaked sample was burned in the tube furnace (Thermolyne 79300) for 1 hour, at operating temperature of 800°C. Nitrogen gas (N_2) was injected into the tube furnace during the activation process, and finally the activated carbon produced was named as 0.4-50 PKSAC. The same method was repeated for 1.4 mm sized PKS biochar and produced 1.4-50 PKSAC. The PKSACs were collected, and the yield were calculated. The morphology of the PKS biochar and PKSACs were observed using field emission scanning electron microscope (FESEM) model JEOL JSM-7900F. The PKSACs were analyzed for the iodine number, pH, bulk density, ash, and moisture content. All the characterization methods were referred to ASTM methods as described by Sinring (2019).

Experimental Design with Response Surface Methodology (RSM)

The adsorption study was conducted via batch mode. To model the removal of both lead ion (Pb^{2+}) and methylene blue (MB), a Box-Behnken design was employed using Design-Expert V12 (Stat-Ease, USA), at three factors, namely initial concentration (5 – 20 ppm for Pb^{2+}, 50 – 250 ppm for MB), pH (4.5 – 7 for Pb^{2+}, 4 – 10 for MB) and contact time (20 – 60 min for Pb^{2+}, 60 – 120 min for MB), were selected as independent variables, and the percentage removal was investigated as a response. Based on the Box-Behnken approach, seventeen experiments were designed, as shown in Table 2 and Table 3.

Lead Ion (Pb^{2+}) Removal

The investigation for Pb^{2+} removal was conducted for two particle sizes of PKSAC (i.e., 0.4 mm and 1.4 mm) using parameters obtained from RSM Box Behnken design. A stock solution of 1000 ppm of Pb^{2+} was diluted into initial concentrations as listed in Table 2 and was transferred into 17 different 250 ml conical flasks. The pH of each Pb^{2+} solution was adjusted to 4.5, 5.75, and 7 using 0.1M HCl or 0.1M KOH, accordingly (Kumar *et al.*, 2011). Then, 1 g of 0.4-50 PKSAC samples were transferred to each conical flask. The mixture was stirred using a magnetic stirrer (Themo Scientific, SP88857105) for

20, 40, and 60 minutes at 400 rpm. After that, the mixture was filtered using filter paper, and the final concentration of the filtrate was determined using Polarized Atomic Absorption Spectrophotometry (Hitachi-Z-5000) at a wavelength of 283.3 nm. The percentage removal of Pb^{2+} was calculated by taking the ratio of the difference between the initial concentration and the final concentration with the initial concentration and multiplied by 100. The same procedures were applied for 1.4-50 PKSAC for Pb^{2+} removal.

Table 2. The Box-Behnken experimental design for Pb^{2+} removal using 0.4-50 PKSAC and 1.4-50 PKSAC

Run	Initial Pb^{2+} Concentration (ppm)	pH	Contact Time (min)
1	5.0	5.75	60
2	5.0	4.50	40
3	5.0	5.75	20
4	5.0	7.00	40
5	12.5	4.50	60
6	12.5	5.75	40
7	12.5	7.00	60
8	12.5	5.75	40
9	12.5	7.00	20
10	12.5	5.75	40
11	12.5	5.75	40
12	12.5	4.50	20
13	12.5	5.75	40
14	20.0	4.50	40
15	20.0	5.75	60
16	20.0	5.75	20
17	20.0	7.00	40

Table 3. The Box Behnken experimental design for MB removal using 0.4-50 PKSAC and 1.4-50 PKSAC

Run	Initial MB Concentration (ppm)	pH	Contact Time (min)
1	50	7.00	60
2	50	4.00	90
3	50	10.00	90
4	50	7.00	120
5	150	7.00	90
6	150	7.00	90
7	150	4.00	120
8	150	7.00	90
9	150	10.00	60
10	150	10.00	120
11	150	7.00	90
12	150	4.00	60
13	150	7.00	90
14	250	7.00	120
15	250	4.00	90
16	250	10.00	90
17	250	7.00	60

Methylene Blue (MB) Removal

The investigation for MB removal was conducted for two particle sizes of PKSAC (i.e., 0.4 mm and 1.4 mm) using parameters obtained from RSM Box Behnken design. A stock solution of 500 ppm of MB was prepared by dissolving 0.5 g of MB powder in 1000 ml distilled water. The stock solution was further diluted using distilled water to 50, 150, and 250 ppm concentration as show in Table 3. 100 ml of the diluted MB solutions were transferred into 17 different 250 ml conical flasks. The pH of the methylene blue solution for each conical flask adjusted to 4, 7, and 10 using 0.1M HCl or 0.1M KOH, accordingly (Kumar *et al*., 2011). Then, 0.2 g of 0.4-50 PKSAC was transferred to each conical flask. The mixture was stirred using a magnetic stirrer for 60, 90, and 120 minutes at 120 rpm. Next, the mixture was filtered using filter paper, and the final concentration of the filtrate was determined using a UV-Vis spectrophotometer at a wavelength of 664 nm. Samples that were too dark were diluted prior to UV-Vis spectrophotometer testing since the equipment cannot read the solutions with high concentration.

RESULT AND DISCUSSION

Percentage Yield of Palm Kernel Shell Activated Carbon (PKSAC)

The percentage yield of PKSAC refers to the amount of PKSAC after the chemical activation of PKS biochar. It is important to note that the temperature for PKS activation was 800°C as this temperature would ensure a high iodine number in the PKSAC according to Sinring (2019). At this temperature, the yield of PKSAC was 55% and 54% for 0.4 mm and 1.4 mm particle sizes treated with 50% KOH, as summarized in Table 4. The mass loss in production of the PKSAC is due to the high activation temperature. This agrees with Rugayah *et al*. (2014), the percentage yield of activated carbon is lower at activation process temperature of 700-800°C. It seems that there is will always be a tradeoff between using high temperatures and yield. It is because to produce activated carbon with high surface area, materials such as volatile matter and carbon materials are burned off (Evans *et al*., 1999; Ip *et al*., 2008). Thus, higher activation temperature results in higher weight loss but also may produce higher surface area. However, the extent of weight loss and surface area depends on the raw material, activating agent used, and temperature.

Characterization of PKSAC (FESEM, Iodine number, pH value, Ash, Moisture, and Bulk Density)

Field emission scanning electron microscope (FESEM) was used to observe the surface morphology of the adsorbents before and after chemical treatment. The FESEM images of PKS biochar and PKSACs were presented in Figure 1. The FESEM images in Figure 1 clearly differentiated the effect of chemical treatment on the porosity of the PKS biochar. PKSACs (Figure 1b and 1c) have excellent pore size, high porosity and rough surfaces, indicating good characteristics to be used as an adsorbent for dye and metal ion uptake (Cheraghi *et al*., 2016). Chemical treatment using KOH affects the surface of PKS biochar to become less smooth with more visible pores, due to dehydration effect of the activating agent (García *et al*., 2017; Islam *et al*., 2017).

Table 4. PKSAC characterization shows the characteristics of 0.4-50 PKSAC and 1.4-50 PKSAC. The iodine number for both the samples were 1209.27 and 1110.13 mg/g, which was on the high end of the range found in commercially available activated carbon shown in Table 1. Examples of commercially available activated carbon. Sinring (2019) stated that the iodine number can be used as an indicator for the porosity of an activated carbon. Activated carbon with high iodine adsorption potential indicates a more mesoporous and microstructure surface area (Yuliusman *et al*., 2017). This was supported by the FESEM micrographs of both PKSACs in Figure 1, in which 0.4-50 PKSAC has better porous structure than 1.4-50 PKSAC. A high iodine number is expected to be able to produce a high

percentage removal of metal ions and dye pigments. In addition, the ash content obtained were 8% and 19% for 0.4-50 PKSAC and 1.4-50 PKSAC, respectively. The lower ash content is preferable as the ability of the adsorption of activated carbon can be affected by the ash content as the ash may block pores. The moisture content of both PKSAC samples were lower than 8%, i.e., less than 5% as stated in the requirements of GAC in AWWA (2012). Activated carbon with high moisture content result in a reduced adsorptive capacity (Zhou *et al.*, 2001). The bulk density of 0.4-50 PKSAC and 1.4-50 PKSAC bulk density value was 0.378 and 0.407 g/mL.

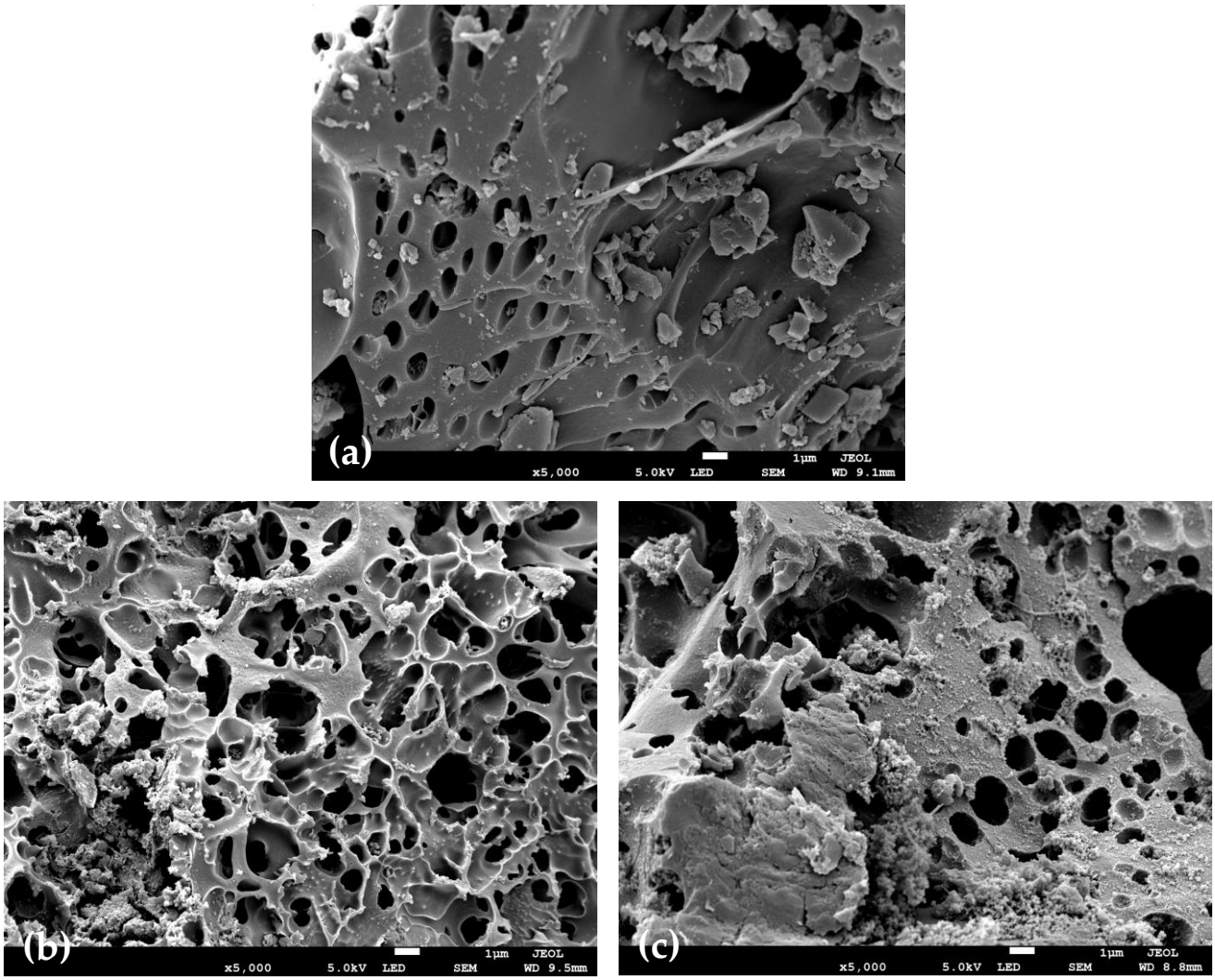

Figure 1. FESEM images at x5,000 magnification (a) PKS biochar (b) 0.4-50 PKSAC (c) 1.4-50 PKSAC

Table 4. PKSAC characterization

Sample Product	0.4-50 PKSAC	1.4-50 PKSAC
Yield (%)	55	54
Iodine Number (mg/g)	1209.27	1110.13
Ash Content (%)	8	19
Moisture Content (%)	2	2.6
Bulk Density (g/mL)	0.378	0.407
pH	7	7

Assessment of Experimental Results with Response Surface Methodology (RSM)

A total of 64 experiments were conducted according to the Box-Behnken experimental design to determine the percentage removal of Pb^{2+} and MB by 0.4-50 PKSAC and 1.4-50 PKSAC at three independent variables. For Pb^{2+} removal, the effects of three independent variables were evaluated: Pb^{2+} initial concentration (5-20 ppm), pH (4.5-7), and contact time (20-60 min). For MB removal, three independent variables were evaluated: MB initial concentration (50-250 ppm), pH (4-10), and contact time (60-120 min). The percentage removal of Pb^{2+} and MB by 0.4-50 PKSAC and 1.4-50 PKSAC were recorded. Four experimental versus predicted graphs (see Figure 2. Experimental versus predicted plot of correlation models for the removal of Pb2+ (a) 0.4-50 PKSAC and (b) 1.4-50 PKSAC2Figure 3) and eight 3D response graphs (see Figure 4 to 7) were obtained from RSM modelling. In RSM, a linear model correlation was best-described the relationship between percentage removal of Pb^{2+} and the three-independent variables. Whereas a quadratic model correlation was best-described the empirical relationships between MB and the three independent variables. These correlation models are shown in the following equations:

Linear Model Correlation:

Percentage removal of Pb^{2+} (0.4-50 PKSAC) = $95.41 + 1.65A + 0.3433B + 0.3514C$

Percentage removal of Pb^{2+} (1.4-50 PKSAC) = $90.71 + 3.23A + 2.15B + 1.74C$

Quadratic Model Correlation:

Percentage removal of MB (0.4-50 PKSAC) = $100.11 - 1.34A - 0.9962B - 1.93AB - 1.26A^2 - 0.5676B^2$

Percentage removal of MB (1.4-50 PKSAC) = $66.35 - 15.98A + 3.54B - 1.13C + 1.74AB - 2.20AC + 6.08BC + 10.46A^2 - 2.68B^2 + 1.10C^2$

The ANOVA F-test and p-values were used to evaluate the statistical significance of the linear, and quadratic correlation models above. The statistical significance of the modelled correlation model was suggested with a condition of greater F-value and low probability value ($p < 0.05$). If the p-values are less than 0.05 (i.e., 95 % confidence level), the effect of the three independent variables on the response was statistically significant. Thus, as shown in Table 5, Table 6 and Table 8, the effects of the three variables on the percentage removal is significant. Whereas if the lack of fit (LOF) was significant, it means the model did not fit the experimental well. As shown in Table 7, the LOF was significant and the model did not fit the experimental data. This would indicate that there is not well-correlate for the removal of MB by 0.4-50 PKSAC as shown in Figure 3(a). However, the models for Pb^{2+} removal using 0.4-50 PKSAC, Pb^{2+} removal using 1.4-50 PKSAC, and MB removal using 1.4-50 PKSAC (Figure 2(a), Figure 2(b), and Figure 3(b), respectively) have shown to be fitting well to the experimental data which means the models developed are adequate.

Table 5. ANOVA for response surface linear model (0.4-50 PKSAC) percentage removal of Pb^{2+}

Response	Source	Sum of Squares	Degree of Freedom	Mean Square	F-Value	p-Value	Comment
Percentage Removal of Pb^{2+} (%)	*Model*	23.69	3	7.90	6.01	0.0085	Significant
	A-Concentration	21.76	1	21.76	16.55	0.0013	
	B-pH	0.9429	1	0.9429	0.7172	0.4124	
	C-Contact Time	0.9895	1	0.9895	0.7527	0.4014	
	Residual	17.09	13	1.31			
	Lack of Fit	9.41	9	1.05	0.5451	0.7935	Not
	Absolute Error	25.12	4	6.28			

Table 6. ANOVA for response surface linear model (1.4-50 PKSAC) percentage removal of Pb^{2+}

Response	Source	Sum of Squares	Degree of Freedom	Mean Square	F-Value	p-Value	Comment
Percentage Removal of Pb^{2+} (%)	*Model*	144.53	3	48.18	12.93	0.0003	Significant
	A-Concentration	83.30	1	83.30	22.35	0.0004	
	B-pH	36.98	1	36.98	9.92	0.0077	
	C-Contact Time	24.25	1	24.25	6.51	0.0242	
	Residual	48.45	13	3.73			
	Lack of Fit	23.33	9	2.59	0.4127	0.8757	Not
	Pure Error	25.12	4	6.28			

Table 7. ANOVA for response surface quadratic model (0.4-50 PKSAC) percentage removal of MB

Response	Source	Sum of Squares	Degree of Freedom	Mean Square	F-Value	p-Value	Comment
Percentage Removal of MB (%)	*Model*	47.57	9	5.29	3.49	0.0568	Not
	A-Concentration	14.31	1	14.31	9.44	0.0180	
	B-pH	0.1035	1	0.1035	0.0683	0.8013	
	C-Contact Time	7.94	1	7.94	5.24	0.0559	
	AB	0.1892	1	0.1892	0.1249	0.7342	
	AC	14.86	1	14.86	9.81	0.0166	
	BC	0.0001	1	0.0001	0.0001	0.9937	
	A^2	7.00	1	7.00	4.62	0.0687	
	B^2	1.80	1	1.80	1.18	0.3124	
	C^2	1.53	1	1.53	1.01	0.3490	
	Residual	10.61	7	1.52			
	Lack of Fit	10.60	3	3.53	2042.36	< 0.0001	Significant
	Pure Error	0.0069	4	0.0017			

Table 8. ANOVA for response surface quadratic model (1.4-50 PKSAC) percentage removal of MB

Response	Source	Sum of Squares	Degree of Freedom	Mean Square	F-Value	p-Value	Comment
Percentage Removal of MB (%)	*Model*	2823.07	9	313.67	9.93	0.0031	Significant
	A-Concentration	2043.84	1	2043.84	64.68	< 0.0001	
	B-Contact Time	100.25	1	100.25	3.17	0.1181	
	C-pH	10.19	1	10.19	0.3225	0.5878	
	AB	12.18	1	12.18	0.3854	0.5544	
	AC	19.40	1	19.40	0.6140	0.4590	
	BC	147.87	1	147.87	4.68	0.0673	
	A^2	460.26	1	460.26	14.56	0.0066	
	B^2	30.29	1	30.29	0.9586	0.3602	
	C^2	5.05	1	5.05	0.1598	0.7012	
	Residual	221.21	7	31.60			
	Lack of Fit	93.99	3	31.33	0.9850	0.4841	Not
	Pure Error	127.22	4	31.80			

TRANSACTIONS ON SCIENCE AND TECHNOLOGY

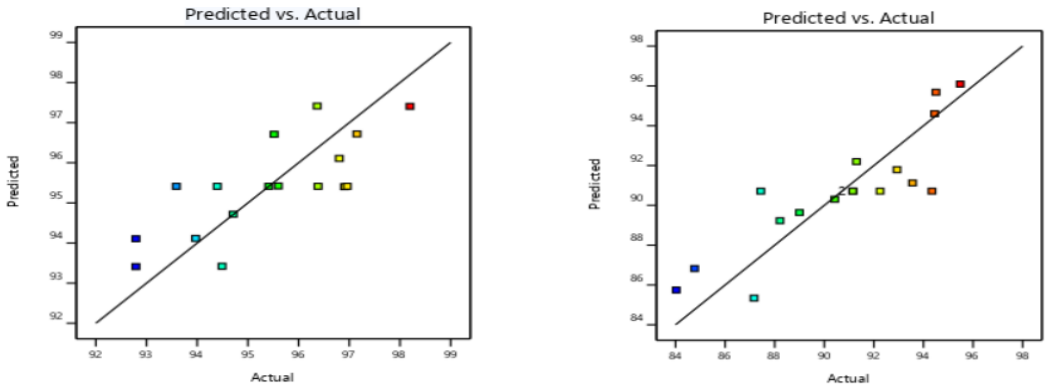

Figure 2. Experimental versus predicted plot of correlation models for the removal of Pb^{2+} (a) 0.4-50 PKSAC and (b) 1.4-50 PKSAC

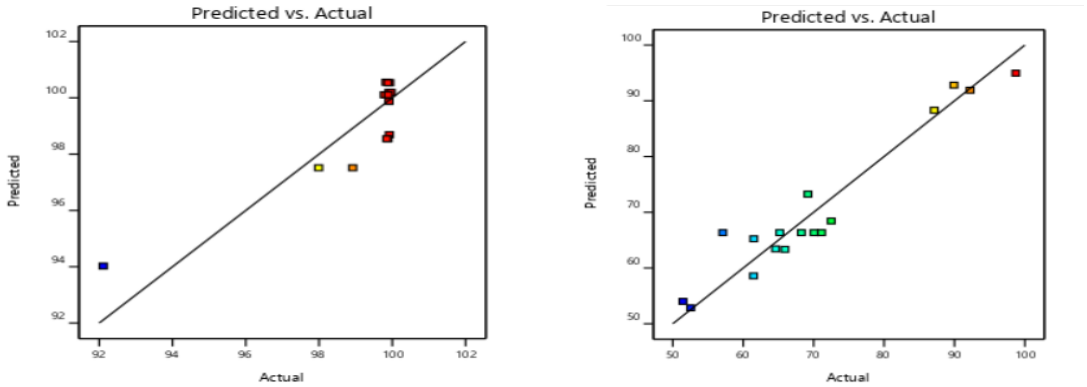

Figure 3. Experimental versus predicted plot of correlation models for the removal of MB (a) 0.4-50 PKSAC and (b) 1.4-50 PKSAC

Summary of Fit Statistics

Table 9 shows the predicted R^2 values for linear and quadratic models for Pb^{2+} removal and MB removal, respectively. The linear models for Pb^{2+} removal was in reasonable agreement with the adjusted R^2 values as the difference between these values were less than 0.2 (Aziz & Aziz, 2018). This means the accuracy for linear model was acceptable. The quadratic models showed R^2 values close to 1.0, showing that the models are within acceptable range (Tran *et al.*, 2017). While the adequate precision indicates the signal to noise (S-N) ratio. Usually, ratios greater than 4 is desirable. For this linear and quadratic model, adequate precision values were higher than 4 which indicates adequate signal for the model to be used effectively to navigate the design space.

Table 9. Fit Statistics (ANOVA)

Sample PKSAC	Model	R^2	Adjusted R^2	Predicted R^2	Adequate Precision
0.4-50 (Pb^{2+})	Linear	0.5799	0.4830	0.3044	7.1784
1.4-50 (Pb^{2+})	Linear	0.6973	0.6275	0.5140	10.0633
0.4-50 (MB)	Quadratic	0.8177	0.3833	-1.9153	7.7415
1.4-50 (MB)	Quadratic	0.9273	0.8339	0.4407	9.7655

Pb^{2+} Percentage Removal

Figure 4 and Figure 5 showed that the percentage removal of Pb^{2+} were above 90% for 0.4-50 PKSAC and above 84% for 1.4-50 PKSAC. It means that both 0.4-50 PKSAC (iodine value of 1209.27 mg/g) and 1.4-50 PKSAC (iodine value of 1110.13 mg/g) were suitable for Pb^{2+} removal with initial Pb^{2+}

concentration of 5 ppm to 20 ppm at pH 4.5 to 7. Pb^{2+} can be easily adsorbed by the activated carbon surface due to its size as its hydrated ionic radii is 4.01 Å (Hen *et al.*, 2010). These results also indicates that the pores within the PKSAC are big enough to allow the diffusion of the Pb^{2+}, as the percentage removal is quite high (86% to >98%) even for the larger particle size 1.4-50 PKSAC. As the initial Pb^{2+} concentration was increased, the percentage removal of Pb^{2+} increased. This may be due to the higher ratio of adsorbent sites to the Pb^{2+} adsorbate at lower initial Pb^{2+} concentration. A further increase of initial Pb^{2+} concentration may result in a maximum percentage removal followed by a decrease in percentage removal, as the ratio of adsorbent sites to the Pb^{2+} adsorbate reduces.

The percentage removal of Pb^{2+} for the 0.4-50 PKSAC is higher than the 1.4-50 PKSAC at varying initial concentration, pH, and contact time. This may be due to the higher iodine number of 0.4-50 PKSAC and more porous structure, which indicated higher surface area. The smaller particle size of 0.4-50 PKSAC may have contributed to higher percentage removal as it has higher surface area to volume ratio at constant mass of activated carbon. This may also be due to a reduced effect of the internal diffusion, (i.e., the rate limiting step) (Wang & Guo, 2020), as the 0.4-50 PKSAC is smaller than the 1.4-50 PKSAC and the diffusion into the pores maybe insignificant. For the larger particle, 1.4-50 PKSAC the internal diffusion becomes a more pronounced rate limiting step, controlling the adsorption. The external diffusion can be assumed not to have any effect on this adsorption as the Pb^{2+} was conducted with 400 rpm agitation.

It is interesting to note that the percentage Pb^{2+} removal shows a slight increase at higher pH and increasing contact time for 0.4-50 PKSAC, but has a higher increase at higher pH and increasing contact time for 1.4-50 PKSAC, as depicted in Figure 4(a) – (b). The increasing percentage removal of Pb^{2+} at higher pH is due to the decreasing of H^+ (Baby & Hussein, 2020). According to Mouni *et al.* (2010) when the concentration of H^+ is lower, the adsorbent surface becomes more negatively charged, thus increasing the attraction between adsorbent and cation. Consequently, increased adsorptive capacity of adsorbent at higher pH (Shrestha *et al.*, 2013).

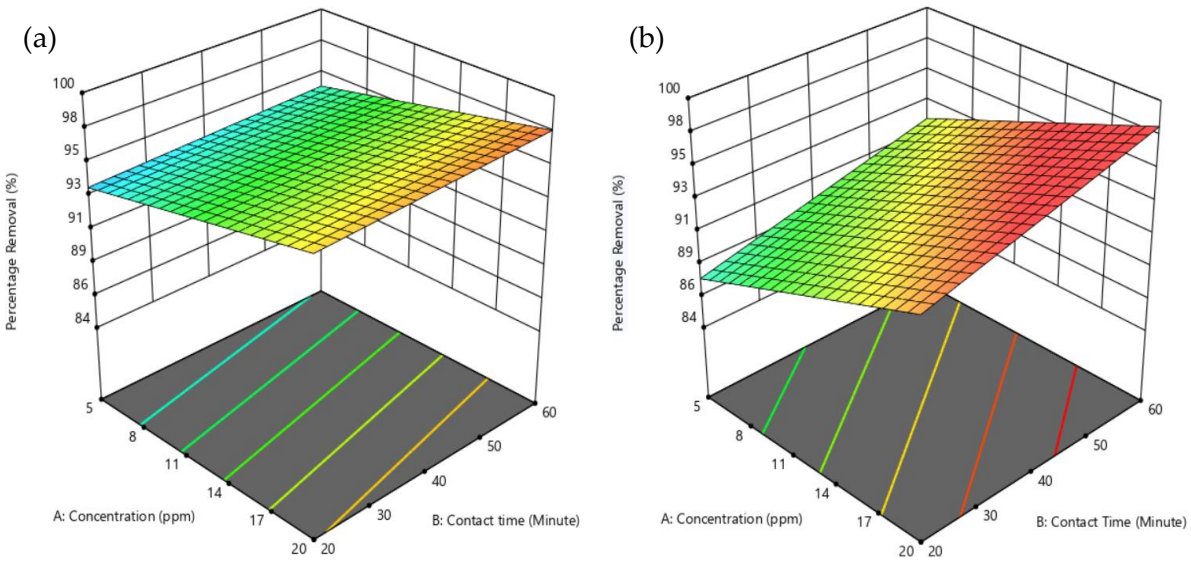

Figure 4. The 3D surface plots related to the interactive effects of concentration and contact time towards percentage removal of Pb^{2+} by (a) 0.4-50 PKSAC and (b) 1.4-50 PKSAC

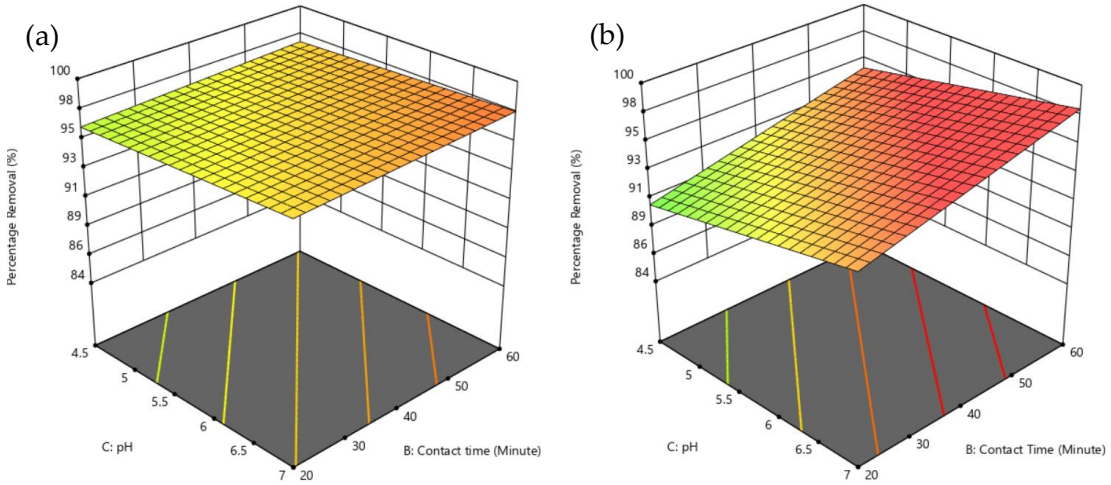

Figure 5. The 3D surface plots related to the interactive effects of pH and contact time towards percentage removal of Pb^{2+} by (a) 0.4-50 PKSAC and (b) 1.4-50 PKSAC

MB Percentage Removal

Figure 6(a) and Figure 7(a) revealed that the percentage removal of MB using 0.4-50 PKSAC is above 90% at varying initial concentration, pH and contact time. This result showed that 0.4-50 PKSAC of iodine number of 1209.26 mg/g was suitable in methylene blue removal. As the iodine number was high, and the PKSAC has small size, both factors contributed to the high surface area of the 0.4-50 PKSAC. This increased the contact surface area with the MB. However, the ANOVA analysis showed that the model for this relationship does not fit well with experimental data. The less significance of the model towards experimental data was well understood from Figure 3(a), in which the predicted and actual values spread out from the linear line.

Figure 6(b) and Figure 7(b) showed that the percentage removal of MB using 1.4-50 PKSAC decreased with increasing initial concentration MB from 50 to 250 ppm. This maybe because, at low MB concentration, the ratio of adsorbent sites to the MB molecules in the solution was close to one, and hence a high percentage of MB molecules may interact with the PKSAC surface and be removed from the solution. But as the initial concentration of MB increased, the ratio of adsorbent sites to MB molecules might be reducing. However, this is unlikely as, MB molecule is much larger than Pb^{2+}, its length is 13.82 Å (Macedo *et al.*, 2006) or 14.47 Å (Dotto *et al.*, 2015), with an approximate width of 9.5 Å. The length depends on the location of the Cl^- on the MB, i.e., it is either connected to the sulfur located in the centre of the molecule or any one of the two nitrogen atoms on the sides (Jia *et al.*, 2018). In view of this, this means the pores on the 1.4-50 PKSAC are large enough for the MB to diffuse into.

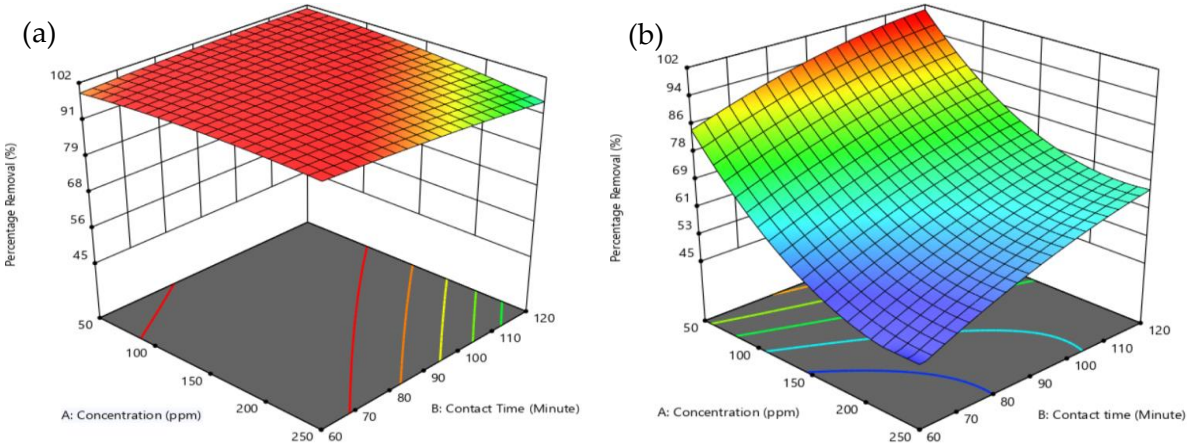

Figure 6. The 3D surface plots related to the interactive effects of concentration and contact time towards percentage removal of MB by (a) 0.4-50 PKSAC and (b) 1.4-50 PKSAC

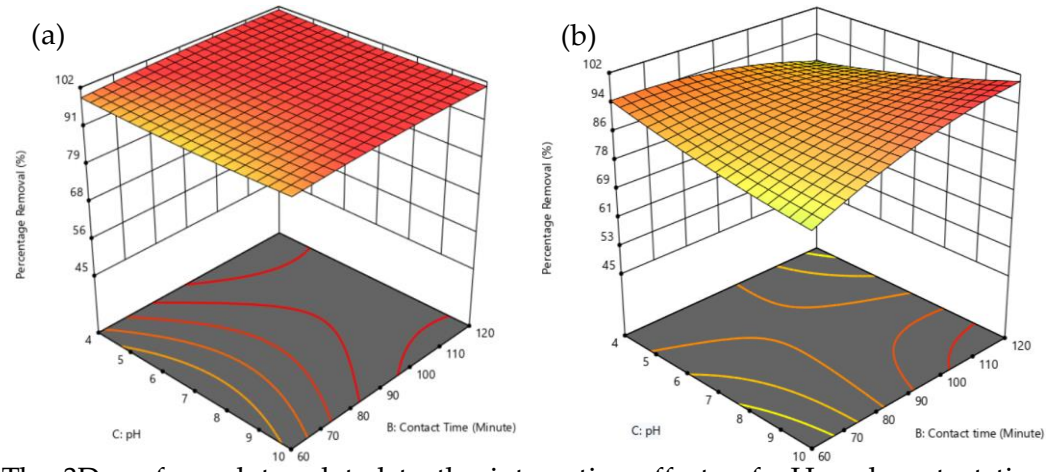

Figure 7. The 3D surface plots related to the interactive effects of pH and contact time towards percentage removal of MB by (a) 0.4-50 PKSAC and (b) 1.4-50 PKSAC

In Figure 6(b) the removal percentage increased with an increase in contact time (60-120 minutes). This may be because as the contact time increased, it gives time for diffusion of the MB molecules in the pores of the PKSAC. As internal diffusion may be a rate limiting step according to Wang & Guo (2020). They reported that external diffusion is also a rate-controlling step. But the agitation conducted in this experiment might have removed that limitation. Figure 7(b) showed that at low pH, the percentage MB removal decreased as the contact time increased but at higher pH the percentage MB removal increased as the contact time increased. This result indicates that there is an optimum contact time for every pH. At high pH, the adsorbent surface is negatively charged, favouring adsorption of cationic dye, such as MB (Khodaie *et al.*, 2013). However, this condition is only applicable for contact time beyond 80 mins. At lower contact time at higher pH, the percentage MB removal slightly reduced, this may be because at these conditions the adsorption equilibrium was not achieved. Meanwhile at low pH with increased contact time, the percentage MB removal will decrease. A reasonable explanation on this phenomenon was due to the competition between excess H^+ ion with MB at low pH (Nsami & Mbadcam, 2013), thus, increasing contact time only lead to a resistance to the diffusion of aggregated MB molecules in the adsorbent, consequently preventing any further adsorption (Utsev *et al.*, 2020).

CONCLUSION

This study showed that PKS biochar with different particle sizes (0.4 mm and 1.4 mm), treated with the same chemical (50% KOH) and conditions (activation at 800°C) to produce 0.4-50 PKSAC and 1.4-50 PKSAC can remove Pb^{2+} and MB. FESEM imaging revealed the change in surface morphology of PKS biochar before and after chemical treatment. The activation process produced 0.4-50 PKSAC and 1.4-50 PKSAC with yield of 55% and 54%, respectively. Table 10 shows the summary of PKSAC characteristics, which were iodine number, ash content, moisture content, bulk density and pH. Then, the interrelated effect of three independent variables on batch adsorption (initial concentration, pH and contact time) were investigated using response surface methodology through the Box-Behnken experimental design (RSM-BB) and were presented in the form of 3D surface responses. The percentage removal was used as the response.

The RSM-BB design linear model correlation for the percentage removal of Pb^{2+} by 0.4-50 PKSAC and 1.4-50 PKSAC was significant. The RSM-BB design quadratic model correlation for the percentage removal of MB by 0.4-50 PKSAC was not significant, however, the fit statistics showed that it was adequate for prediction. While the quadratic model correlation for percentage removal of MB by 1.4-

50 PKSAC was significant. Using the models, time and cost can be saved as the percentage removal of Pb^{2+} or MB by 0.4-50 PKSAC or 1.4-50 PKSAC could be predicted, under stated conditions.

Table 10. Summary on characterization of PKSACs

Sample Product		0.4-50 PKSAC	1.4-50 PKSAC
Yield (%)		55	54
Characterization	Iodine Number (mg/g)	1209.27	1110.13
	Ash Content (%)	8	19
	Moisture Content (%)	2	2.6
	Bulk Density (g/mL)	0.378	0.407
	pH	7	7

The experimental adsorption percentage of Pb^{2+} by 0.4-50 PKSAC and 1.4-50 PKSAC showed a maximum removal of 98.20% and 95.48%, respectively at conditions of 60 min contact time, initial Pb^{2+} concentration of 20 ppm, pH 7, at room temperature, and agitation speed of 400 rpm. On the other hand, the experimental adsorption percentage of MB by 0.4-50 PKSAC and 1.4-50 PKSAC showed a maximum removal of 99.97% and 98.71%, respectively at conditions of 90 min contact time, initial MB concentration of 50 ppm with pH 10, at room temperature, and agitation speed of 120 rpm. These could be the best conditions for Pb^{2+} and MB removal for both sizes of PKSACs, since the percentage removal were greater than 95%. The removal ability of PKSAC indicated that the pore size was able to accommodate Pb^{2+} (4.01 Å) and the MB (14.47 Å, width 9.5 Å).

ACKNOWLEDGEMENTS

The authors want to fully acknowledge Universiti Malaysia Sabah and Borneo Energy Sdn. Bhd. for their collaboration.

REFERENCES

[1] Abdul Rahman, A., Sulaiman, F. & Abdullah, N. 2016. Influence of washing medium pre-treatment on pyrolysis yields and product characteristics of palm kernel shell. *Journal of Physical Science*, 27(1), 53–75.

[2] AWWA. 2012. *Granular Activated Carbon: AWWA Standard B604-12*. Compiled by A. N. S. Institute. New York, USA: American Water Works Association.

[3] Aziz, A. R. A. & Aziz, S. A. 2018. Application of Box Behnken Design to Optimize the Parameters for Kenaf-Epoxy as Noise Absorber. *Proceedings of the 1st International Conference on Materials Engineering and Science (IConMEAS 2018)*. 8 August, 2018. Istanbul, Turkey. pp 012001.

[4] Baby, R. & Hussein, M. Z. 2020. Ecofriendly Approach for Treatment of Heavy-Metal-Contaminated Water Using Activated Carbon of Kernel Shell of Oil Palm. *Materials*, 13(11), 11–13.

[5] Biswas, S. & Mishra, U. 2015. Continuous Fixed-Bed Column Study and Adsorption Modeling: Removal of Lead Ion from Aqueous Solution by Charcoal Originated from Chemical Carbonization of Rubber Wood Sawdust. *Journal of Chemistry*, 2015, 907379.

[6] Cheraghi, E., Ameri, E. & Moheb, A. 2016. Continuous biosorption of Cd(II) ions from aqueous solutions by sesame waste: thermodynamics and fixed-bed column studies. *Desalination and Water Treatment*, 57(15), 6936–6949.

[7] Dotto, G. L., Santos, J. M. N., Rodrigues, I. L., Rosa, R., Pavan, F. A. & Lima, E. C. 2015. Adsorption of Methylene Blue by Ultrasonic Surface Modified Chitin. *Journal of Colloid and Interface Science*, 446, 133–140.

[8] Evans, M. J. B., Halliop, E. & MacDonald, J. A. F. 1999. The production of chemically-activated carbon. *Carbon*, 37, 269–274.

[9] García, J. R., Sedran, U., Abbas, M., Zaini, A. & García, J. R. 2017. Preparation, characterization, and dye removal study of activated carbon prepared from palm kernel shell. *Environmental Science and Pollution Research*, 25, 5076–5085.

[10] Hen, S. B. C., Hen, L. C. & Ian, K. X. 2010. Adsorption of aqueous Cd^{2+} , Pb^{2+} , Cu^{2+} ions by nano-hydroxyapatite: Single- and multi-metal competitive adsorption study. *Geochemical Journal*, 44, 233–239.

[11] Huang, Y., Wu, D., Wang, X., Huang, W., Lawless, D. & Feng, X. 2016. Removal of heavy metals from water using polyvinylamine by polymer-enhanced ultrafiltration and flocculation. *Separation and Purification Technology*, 158, 124–136.

[12] Ip, A. W. M., Barford, J. P. & McKay, G. 2008. Production and comparison of high surface area bamboo derived active carbons. *Bioresource Technology*, 99, 8909–8916.

[13] Islam, M. A., Ahmed, M. J., Khanday, W. A., Asif, M. & Hameed, B. H. 2017. Mesoporous activated coconut shell-derived hydrochar prepared via hydrothermal carbonization-NaOH activation for methylene blue adsorption. *Journal of Environmental Management*, 203, 237–244.

[14] Jia, P., Tan, H., Liu, K. & Gao, W. 2018. Removal of Methylene Blue from Aqueous Solution by Bone Char. *Applied Sciences*, 8(10), 1903.

[15] Khodaie, M., Ghasemi, N., Moradi, B. & Rahimi, M. 2013. Removal of Methylene Blue from Wastewater by Adsorption onto $ZnCl_2$ Activated Corn Husk Carbon Equilibrium Studies. *Journal of Chemistry*, 2013, 383985.

[16] Kumar, P. S., Ramalingam, S. & Sathishkumar, K. 2011. Removal of methylene blue dye from aqueous solution by activated carbon prepared from cashew nut shell as a new low-cost adsorbent. *Korean Journal of Chemical Engineering*, 28(1), 149–155.

[17] Macedo, J. D. S., Bezerra, N., Almeida, L. E., Fragoso, E., Cestari, A. R., Gimenez, I. D. F., Lênin, N., Carreño, V. & Barreto, L. S. 2006. Kinetic and calorimetric study of the adsorption of dyes on mesoporous activated carbon prepared from coconut coir dust. *Journal of Colloid and Interface Science*, 298, 515–522.

[18] Mohamad Salleh, Z. N. 2010. *To Produce the Activated Carbon from Matured Palm Kernel Shell*. BEng Thesis, Universiti Malaysia Pahang, Malaysia.

[19] Mouni, L., Merabet, D., Bouzaza, A. & Belkhiri, L. 2010. Removal of Pb^{2+} and Zn^{2+} from the aqueous solutions by activated carbon prepared from Dates stone. *Desalination and Water Treatment*, 16(1–3), 66–73.

[20] Nsami, J. N. & Mbadcam, J. K. 2013. The Adsorption Efficiency of Chemically Prepared Activated Carbon from Cola Nut Shells by $ZnCl_2$ on Methylene Blue. *Journal of Chemistry*, 2013, 469170.

[21] Rashidi, N. A. & Yusup, S. 2019. Production of palm kernel shell-based activated carbon by direct physical activation for carbon dioxide adsorption. *Environmental Science and Pollution Research*, 26(33), 33732–33746.

[22] Rugayah, A. F., Astimar, A. A. & Norzita, N. 2014. Preparation and Characterisation of Activated Carbon from Palm Kernel Shell by Physical Activation with Steam. *Journal of Oil Palm Research*, 26(3), 251–264.

[23] Saleem, J., Shahid, U. Bin, Hijab, M., Mackey, H. & McKay, G. 2019. Production and applications of activated carbons as adsorbents from olive stones. *Biomass Conversion and Biorefinery*, 9, 775–802.

[24] Shrestha, R. M., Pradhananga, R. R., Varga, M. & Varga, I. 2011. Preparation of Activated Carbon for the Removal of Pb(II) from Aqueous Solutions. *Journal of Nepal Chemical Society*, 28, 94–101.

[25] Sinring, N. 2019. *Production of Commercial Grade Granular Activated Carbon From Vacuum Pyrolysis Biochar Via Chemical Activation*. BEng Thesis, Universiti Malaysia Sabah, Malaysia.

[26] Tran, T. Van, Bui, Q. T. P., Nguyen, T. D., Le, N. T. H. & Bach, L. G. 2017. A comparative study on the removal efficiency of metal ions (Cu^{2+}, Ni^{2+}, and Pb^{2+}) using sugarcane bagasse-derived $ZnCl_2$-activated carbon by the response surface methodology. *Adsorption Science & Technology*, 35(1–2), 72–85.

[27] Utsev, J. T., Iwar, R. T. & Ifyalem, K. J. 2020. Adsorption of Methylene Blue from Aqueous Solution onto Delonix regia Pod Activated Carbon: Batch Equilibrium Isotherm, Kinetic and Thermodynamic Studies. *Journal of Materials and Environmental Science*, 11(7), 1058–1078.

[28] Wang, J. & Guo, X. 2020. Adsorption kinetic models: Physical meanings, applications, and solving methods. *Journal of Hazardous Materials*, 390(May), 122156.

[29] Yuliusman, Nasruddin, Afdhol, M. K., Amiliana, R. A. & Hanafi, A. 2017. Preparation of Activated Carbon from Palm Shells using KOH and $ZnCl_2$ as the Activating Agent. *Proceedings of the International Conference on Green and Renewable Energy Resources (ICGRER 2016)*. 14-15 November, 2016. Solo, Indonesia. pp 012009.

[30] Zhou, L., Li, M., Sun, Y. & Zhou, Y. 2001. Effect of moisture in microporous activated carbon on the adsorption of methane. *Carbon*, 39, 773–776.